Selection Transmitting/Maximum Ratio Combining for Timing Synchronization of MIMO-OFDM Systems

Jianhua Zhang, Lei Tian, Yuning Wang, and Mengmeng Liu

***Abstract*—In multiple-input multiple-output orthogonal frequency division multiplexing (MIMO-OFDM) systems, timing synchronization is important in order to find the correct start of OFDM frames and symbols at the receiver. In this paper, a joint transmit antenna selection and maximum ratio combining at the receiver (ST/MRC) are proposed to improve the timing synchronization performance of MIMO-OFDM systems. In this scheme, only the antenna with the highest channel power is selected at the transmitter. The timing metrics of all receive antennas are added together to realize maximum ratio combining (MRC). In order to theoretically investigate the performance of the proposed scheme, the timing metric based on a time-domain repetitive synchronization sequence structure is adopted and the closed-form expression for the correct timing probability (CTP) in the flat fading channel is derived. Then the proposed ST/MRC scheme for timing synchronization is applied in multipath fading channels. The advantage of the proposed scheme for timing synchronization is verified by simulations.**

***Index Terms*—OFDM, MIMO, diversity, synchronization, timing.**

I. Introduction

ORTHOGONAL Frequency Division Multiplexing (OFDM) has been widely accepted as one of the most important techniques for the wireless communication and broadcasting systems [1], e.g., IEEE802.11, IEEE802.16, digital audio broadcasting (DAB) and digital video broadcasting terrestrial (DVB-T) [2]–[5]. By inserting a cyclic prefix (CP) before each transmitted symbol, OFDM system increases its robustness against the inter-symbol interference (ISI) caused by multipath fading channels. Moreover, OFDM can be combined with multiple antennas at both transmitter and receiver to achieve diversity gain and to enhance the system capacity over the fading channel, which results in a MIMO-OFDM system [6]–[9].

This work was supported in part by the National Natural Science Foundation of China under Grants 61171105 and 61322110, the National Key Technology Research and Development Program of the Ministry of Science and Technology of China under Grant 2012BAF14B01, the National 863 Project of the Ministry of Science and Technology under Grants 2014AA01A705 and 2014AA01A706, the Program for New Century Excellent Talents in University of Ministry of Education of China under Grant NCET-11-0598, and the Research Fund for the Doctoral Program of Higher Education under Grant 20130005110001.

J. Zhang, L. Tian, Y. Wang and M. Liu are with the Key Laboratory of Universal Wireless Communications, Ministry of Education, Beijing University of Posts and Telecommunications, Beijing, China (e-mail: jhzhang@bupt.edu.cn; tianlbupt@gmail.com; yuning.wang11@gmail.com; liumm.bupt@hotmail.com). The corresponding author is J. Zhang (e-mail: jhzhang@bupt.edu.cn).

Incorrect timing estimation will degrade the system performance severely due to the introduction of ISI and inter-carrier-interference (ICI). Timing synchronization aims at finding the start of OFDM frames and symbols at the receiver. MIMO-OFDM systems are more sensitive to synchronization errors compared with single-input single-output (SISO)-OFDM systems [10]–[18]. Therefore, timing synchronization plays a pivotal role in the receiver design for MIMO-OFDM systems. [14] is the pioneering work to explore the synchronization in SISO-OFDM systems. By detecting upon the receipt of one training sequence consisting of two symbols, the start of the frame and the beginning of the symbol can be acquired rapidly and robustly. Recently, [15] carries out research about timing synchronization over multipath fading channels. The target of timing synchronization in multipath fading channels is to search for the first path. By utilizing the characteristics of the differential cross correlation between the training sequences, all possible multiple taps can be found. Then threshold based fine timing is applied to search for the first tap among multiple delay taps. With respect to MIMO-OFDM systems, various diversity schemes have been discussed in the literature to improve the synchronization performance [19]–[23]. But most of them focus on the estimation and correction of the carrier frequency offset (CFO), which results from the imperfect oscillator between the transmitter and the receiver. The receiver diversity scheme for timing synchronization is firstly proposed in [20]. References [21] and [22] present timing synchronization by Schmidl-Cox correlation with equal gain combining (EGC) and maximum ratio combining (MRC) at the receiver.

While the receiver diversity for the timing synchronization has been investigated in the literature, the application of various transmitter diversity schemes for the timing synchronization has not been exploited yet. Only maximum ratio transmitting (MRT) for the packet detection is proposed and it is realized by adopting the orthogonal synchronization training sequences at the transmitter [21]. The number of radio frequency (RF) chains in conventional MIMO systems is equal to the total number of antennas, which has stringent requirements for the hardware design and is of high cost. Therefore, selection transmitting (ST) is a reasonable choice at the transmitter to minimize the use of RF chains. It has been proved that selection transmitting can efficiently increase the link performance [24]. Moreover, selection transmitting at the transmitter can be combined with maximum ratio combining at the receiver to form ST/MRC. It has been verified that the

outage probability of ST/MRC is proportional to the product of number of transmit and receive antennas and full diversity order is achieved for data transmission [25]–[27]. Up to now, to the best of our knowledge, there is no paper applying ST/MRC in timing synchronization of MIMO-OFDM systems. Thus considering the advantages of ST and MRC, we bridge the gap between ST/MRC scheme and timing synchronization in this paper.

Moreover, this scheme is very suitable for the uplink scenario of interactive broadcasting systems, since only one RF chain is needed, then the cost and hardware limitations of the transmitter are overcome [8]. Thus, the application of ST/MRC will improve the timing performance and decrease the hardware cost. In this paper, by defining the correct timing probability (CTP), we derive the closed-form expression for timing synchronization with ST/MRC. The analysis shows that ST/MRC scheme can achieve a full diversity order for the timing synchronization, thus improving the timing performance greatly. Then the theoretical results for different antenna configurations are compared. Finally we validate our theoretical analysis by simulation results.

The main contribution of this paper is summarized as follows.

1) This paper firstly applies ST/MRC scheme in the timing synchronization of MIMO-OFDM systems. Specifically, at the transmitter only one out of multiple transmit antennas with the maximal total channel power at the receiver is selected to transmit the synchronization training sequence. The timing metric is defined as the correlation between the received synchronization sequence and the corresponding complex conjugated version. Then, at the receiver, the timing metric for each receive antenna is combined coherently based on the MRC scheme. Thus, the timing metric peak which indicates the beginning of the frame can be detected with an obviously improved signal-to-noise ratio (SNR).
2) The closed-form expressions for CTP and error timing probability (ETP) with ST/MRC, ST only, MRT only and MRC only in the flat fading channel are derived, respectively. The mathematical expression proves that the proposed ST/MRC scheme for timing synchronization can achieve the full diversity order. Thus, the timing performance can be greatly enhanced. These analytical conclusions are also validated by simulations.
3) The timing synchronization by utilizing the ST/MRC scheme in the multipath channel is also investigated. Different from the timing detection in the flat fading channel, there are more than one timing metric peaks in the multipath channel, which are caused by the multiple channel delay taps. It is necessary to empirically search for the first arrival path after utilizing the ST/MRC scheme. The timing performance with the ST/MRC scheme in the multipath channel is evaluated by simulations.

The rest of the paper is organized as follows. Section II describes the MIMO-OFDM system model with the timing synchronization module. Section III covers the theoretical analysis of timing synchronization performance for the proposed ST/MRC scheme in flat fading channels. Section IV presents the application of ST/MRC scheme for timing synchronization in multipath fading channels. Section V demonstrates the simulation results. Finally the conclusions are achieved.

Notation: boldface letters are used for matrices and vectors; $()^T$, $()^*$ and $()^H$ represent transpose, complex conjugate and Hermitian (conjugate) transpose respectively; $\mathbf{I}_N$ represents $N\times N$ identity matrix. $[\cdot]_{i,j}$ denotes $i\times j$ entry of a matrix; $\delta(t)$ is Dirac function; $|\cdot|$ is modulus; $f(\cdot)$ means function; $\max(\cdot)$ denotes maximum; $\Gamma(n) = (n-1)!$ is fractional function; $j = \sqrt{-1}$; $\mathbb{E}(\cdot)$ is expectation of a random variable. Finally, $\forall$ denotes any and $\mathrm{floor}(A)$ indicates that the element of A is rounded to the nearest integers less than or equal to A.

II. System Model

Fig. 1 shows the structure diagram of the ST/MRC scheme for the timing synchronization in a MIMO-OFDM system with N_t transmit antennas and N_r receive antennas. The timing recovery at the receiver relies on searching for the synchronization training sequence preceding each transmission frame as illustrated in Fig. 2. The synchronization sequence in the frequency domain is denoted as $\mathbf{C}$ with one OFDM symbol length N. The odd subcarriers are forced to zeros, i.e., $\mathbf{C} = \{C(0), 0, C(1), 0, C(2), \ldots, C(N/2-1), 0\}^T$ [14]. Then after N-point inverse fast Fourier transform (IFFT), the synchronization training sequence in the time domain consists of two identical halves, which is represented as:

$$\left[\begin{array}{c} \mathbf{c} \\ \mathbf{c} \end{array}\right] = \sqrt{2}\mathbf{W}\mathbf{C}, \tag{1}$$

where $\mathbf{c}$ is an $N/2\times 1$ column vector and (1) denotes that the synchronization training sequence has two identical halves in the time domain; $\sqrt{2}$ is used to normalize the power of the synchronization training sequence after zeros padding; $\mathbf{W}$ is the $N\times N$ IFFT transform matrix with entry $e^{j2\pi nk/N}$ at the n-th row and the k-th column.

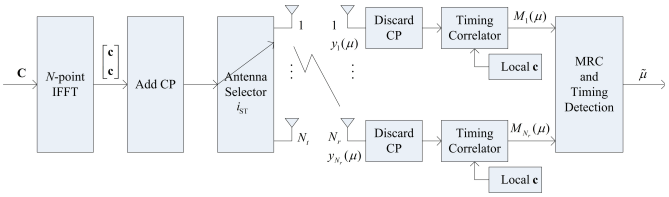

Fig. 1. Structure diagram of ST/MRC for timing synchronization in a MIMO-OFDM system

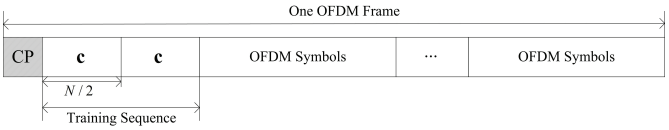

Fig. 2. The frame structure

After cyclic prefix (CP) padding, digital to analog converter (DAC) and RF module, the two identical halves are transmitted over the MIMO flat fading channel. Let $h_{i,k}$ represent

the channel state information (CSI) from the i-th transmit antenna to the k-th receive antenna, which are modeled as the independent identically distributed (i.i.d.) complex Gaussian random variable with zero mean and the variance of 0.5 per dimension. The amplitude of the flat fading channel $|h_{i,k}|$ is Rayleigh distributed, thus, the channel power $|h_{i,k}|^2$ obeys the exponential distribution as:

$$p_{|h_{i,k}|^2}(x) = e^{-x},\ x \geq 0. \tag{2}$$

It is well known that the MRC scheme is to add the independent fading channels associated with each receive antenna coherently. We would like to utilize the MRC scheme at the receiver to improve the timing performance. At the same time, at the transmitter only a single transmit antenna with the maximal total received channel power at the receiver, denoted as i_{ST}, is selected out of N_t transmit antennas, which is mathematically represented as:

$$i_{\mathrm{ST}} = \underset{1\leq i\leq N_t}{\arg\max} \left(T_i = \sum_{k=1}^{N_r} |h_{i,k}|^2 \right), \tag{3}$$

where T_i is the sum of the channel power between each receive antenna and the i-th transmit antenna. The selection is performed at the receiver. Only the value of i_{ST} is sent back to the transmitter through a feedback channel. For example, only one-bit overhead is feedback to the transmitter in the two-antenna scenario and two-bit overhead is required for feedback in the four-antenna scenario. It is assumed that there is no feedback delay or error.

In the flat Rayleigh MIMO channel, T_i is i.i.d. chi-squared random variable with $2N_r$ degrees of freedom. Its cumulative distribution function (c.d.f.) is given by Eq. (7.19) in [28]:

$$P_{T_i}(x) = 1 - e^{-x} \sum_{k=0}^{N_r-1} \frac{x^k}{\Gamma(k+1)},\ x \geq 0. \tag{4}$$

Therefore, the probability density function (p.d.f.) of $T_{i_{\mathrm{ST}}}$ is given by Eq. (7.9) in [28]:

$$p_{i_{\mathrm{ST}}}(x) = \frac{N_t}{\Gamma(N_r)} \left(1 - e^{-x} \sum_{k=0}^{N_r-1} \frac{x^k}{\Gamma(k+1)} \right)^{N_t-1} x^{N_r-1} e^{-x}. \tag{5}$$

After passing through the channel, the received synchronization sequence at the k-th receive antenna from the selected i_{ST} transmit antenna is mathematically represented as:

$$y_k(\mu) = h_{i_{\mathrm{ST}},k} c(\mu - \hat{\mu}) + w_k(\mu), \tag{6}$$

where μ is the discrete time shift, $\hat{\mu}$ is the desired timing indicating the beginning of the frame and the start of the OFDM symbol. Our target is to estimate the desired timing by utilizing ST/MRC scheme and the synchronization training sequence. w_k represents the complex additive white Gaussian noise (AWGN) with a zero mean and the variance σ^2. In this paper, we assume that the fading channel varies slowly, remains constant within one frame and changes continuously from one frame to another.

III. Correct Timing Probability of ST/MRC Scheme

In this section, we will present the definition of the timing metric and estimate the timing shift in order to finish the timing synchronization at the receiver. The timing metric for the k-th receive antenna is defined as the correlation between the received two identical halves and the local complex conjugated versions, which is shifted by $N/2$ samples [29]:

$$M_k(\mu) = \left[\sum_{d=0}^{N/2-1} c^*(d) y_k(\mu + d) \right]^* \times \left[\sum_{m=0}^{N/2-1} c^*(m) y_k \left(\mu + m + \frac{N}{2} \right) \right], \tag{7}$$

where $N/2$ is the size of the correlation window. Substituting (6) into (7), the timing metric for the k-th receive antenna can be rewritten as:

$$M_k(\mu) = \left[h_{i_{\mathrm{ST}},k} \sum_{d=0}^{N/2-1} c^*(d) c(\mu - \hat{\mu} + d) + \eta_{k,1}(\mu) \right]^* \times \left[h_{i_{\mathrm{ST}},k} \sum_{m=0}^{N/2-1} c^*(m) c \left(\mu - \hat{\mu} + m + \frac{N}{2} \right) + \eta_{k,2}(\mu) \right], \tag{8}$$

where $\eta_{k,1}(\mu) \triangleq \sum_{d=0}^{N/2-1} c^*(d) w_k(\mu + d)$ and $\eta_{k,2}(\mu) \triangleq \sum_{m=0}^{N/2-1} c^*(m) w_k \left(\mu + m + \frac{N}{2} \right)$ are with a zero mean and the variance $N\sigma^2/2$. Considering the orthogonality of the synchronization training sequence [1], i.e., $\sum_{d=0}^{N/2-1} c^*(d) c(\mu + d) = \frac{N}{2}\delta(\mu)$, (8) can be rewritten as:

$$M_k(\mu) = \left[\frac{N}{2} h_{i_{\mathrm{ST}},k} \delta(\mu - \hat{\mu}) + \eta_{k,1}(\mu) \right]^* \times \left[\frac{N}{2} h_{i_{\mathrm{ST}},k} \delta(\mu - \hat{\mu}) + \eta_{k,2}(\mu) \right] \tag{9}$$

After the mathematical manipulation, (9) is simplified as:

$$M_k(\mu) = \underbrace{\left(\frac{N}{2} \right)^2 |h_{i_{\mathrm{ST}},k}|^2 \delta(\mu - \hat{\mu})}_{\text{useful signal}} + \underbrace{\eta^*_{k,1}(\mu)\eta_{k,2}(\mu)}_{2_{\mathrm{nd}}-\text{order noise}} + \underbrace{\frac{N}{2} h_{i_{\mathrm{ST}},k} \eta^*_{k,1}(\mu)\delta(\mu - \hat{\mu}) + \frac{N}{2} h^*_{i_{\mathrm{ST}},k} \eta_{k,2}(\mu)\delta(\mu - \hat{\mu})}_{1_{\mathrm{st}}-\text{order noise}}. \tag{10}$$

From (10), it is observed that when the received synchronization sequence correlates with the local synchronization sequence to the maximal extent, the timing metric $M_k(\mu)$ generates a peak value but is degraded by the noise. Furthermore, the coefficient of the useful signal at each receive antenna is

[1] If the auto correlation function (ACF) of the synchronization sequence is not ideal, the self-interference term will appear, which will degrade the timing detection performance. However, the self-interference cancelation scheme can be used to improve the timing performance because the interference caused by non-ideal ACF appears at the fixed known position [30]. Moreover, the proposed ST/MRC scheme only needs one synchronization sequence at the transmitter and looses the requirement for cross-correlation of synchronization sequence. Thus the ideal ACF is assumed here for analysis.

related to the sum of channel powers between the selected transmit antenna and each receive antenna, which inspires us to utilize the MRC scheme to improve the power of the useful signal at the desired timing position. Thus, we combine the timing metric for each receive antenna coherently, which is presented as:

$$M_{\mathrm{MRC}}(\mu) = \sum_{k=1}^{N_r} M_k(\mu). \tag{11}$$

Next, the timing shift could be detected based on the timing metric with an aggregated SNR level. In the flat fading channel, timing detection is quite straightforward. The time index with the highest power in the absolute value of the timing metric is selected as the estimated timing shift, which is mathematically expressed as:

$$\tilde{\mu} = \underset{-N/2 \le \mu \le N/2-1}{\arg\max} \left| M_{\mathrm{MRC}}(\mu) \right|. \tag{12}$$

Then the estimated $\tilde{\mu}$ is forwarded to decode the frame further. Fig. 3 shows an example of the absolute value of the timing metric for 1×1 antenna configuration under the one path spatial channel model (SCM) with the speed of 3 km/h and SNR $= 0$ dB [31]. Each frame is comprised of 2 OFDM symbols. The first symbol is the synchronization training sequence. Because a single antenna is selected at the transmitter in our proposed scheme, only one synchronization sequence is required. Frank-Zadoff-Chu code with length $N_{\mathrm{CP}} = 64$ is adopted as the synchronization sequence. The simulation parameters are listed in Table I.

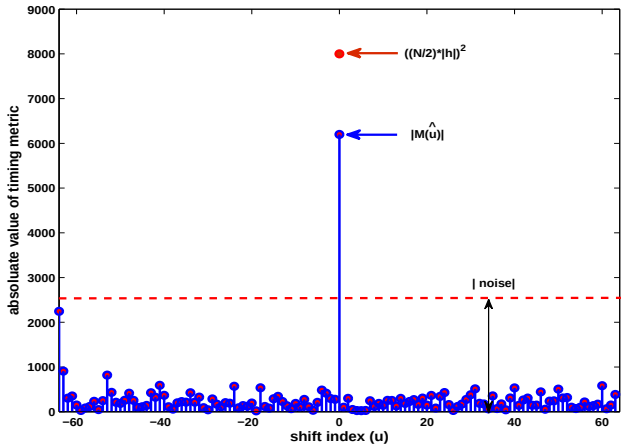

Fig. 3. One example of the absolute values of timing metric over 1×1 flat fading channel

Fig. 3 clearly shows the correct beginning of the frame corresponding to the time index $\hat{\mu} = 0$ where the peak $|M_1(\mu)|$ locates at (indicated by the blue arrow). The value of the useful signal locating at the desired timing position $\hat{\mu}$ is also plotted in Fig. 3, which is indicated by the red arrow. It is noted that $|M_1(\mu)|$ is lower than the useful signal. The reason is that the timing metric peak is degraded by the first and second order noises as shown in (10). There is the second order noise at other time shift positions. It is observed that the second order noise is much lower than the first order noise. Thus it is reasonable to omit the higher order noise for simplicity in the following analysis.

However, due to the time-variant fading property of the channel and the variation of the noise, it is possible that the useful signal $\left(\frac{N}{2}\right)^2 |h_{i_{\mathrm{ST}},k}|^2$ is lower than the first-order noise. Then the beginning of the frame cannot be detected correctly, i.e., $\tilde{\mu} \neq \hat{\mu}$. In order to describe the probability of the correct timing detection quantitatively, we define the correct timing probability (CTP) and derive the analytical CTP expressions for some typical diversity schemes in the subsequent sections.

A. $N_t = 1$ and $N_r = 1$

In this case, by ignoring the second order noise, the absolute value of the timing metric in (10) is simplified as

$$|M_1(\mu)| \approx \left| \left(\frac{N}{2}\right)^2 |h_{1,1}|^2 \delta(\mu - \hat{\mu}) + \frac{N}{2} \left[h_{1,1}\eta_{1,1}^*(\mu) + h_{1,1}^*\eta_{1,2}(\mu) \right] \delta(\mu - \hat{\mu}) \right|. \tag{13}$$

Notice that the useful signal is the real value with the amplification factor $\left(\frac{N}{2}\right)^2$. Thus the noise term in $|M_1(\mu)|$ is much lower than the useful signal in the high SNR regime. Then (13) can be approximately expressed as:

$$|M_1(\mu)| \approx \left(\frac{N}{2}\right)^2 |h_{1,1}|^2 \delta(\mu - \hat{\mu}) + \frac{N}{2} \left| h_{1,1}\eta_{1,1}^*(\mu) + h_{1,1}^*\eta_{1,2}(\mu) \right| \delta(\mu - \hat{\mu}). \tag{14}$$

On the basis of (14), we define two new random variables as

$$U = \left(\frac{N}{2}\right)^2 |h_{1,1}|^2, \; V = \frac{N}{2} \left| h_{1,1}\eta_{1,1}^*(\hat{\mu}) + h_{1,1}^*\eta_{1,2}(\hat{\mu}) \right|, \tag{15}$$

which denote the useful signal and the noise respectively. The two variables change with time from one frame to another. Then we introduce a new random variable Z, which is the useful signal divided by the noise, i.e.,

$$Z = \frac{U^2}{V^2} = \frac{\left(\frac{N}{2}\right)^4 |h_{1,1}|^4}{\left(\frac{N}{2}\right)^2 \left| h_{1,1}\eta_{1,1}^*(\hat{\mu}) + h_{1,1}^*\eta_{1,2}(\hat{\mu}) \right|^2}. \tag{16}$$

As analyzed before, only when the useful signal U emerges from the dominating first order noise V, the estimated timing shift in (12) is the correct timing estimation where the true beginning of the OFDM frame locates in. That is the desired timing can be acquired. Based on the analysis above, we define the correct timing probability of 1×1 antenna configuration as the probability that Z is larger than one. That is $P(Z > 1)$. It is noted that the closed-form expression for CTP in MIMO systems is related to the distribution of Z. But it is hard to derive this distribution due to the division operation in the definition of Z. In order to make this problem tractable, we utilize the average power (AP) of the noise. That is the statistic characteristic of V^2, which is mathematically represented as:

$$\mathbb{E}\{V^2\} = \left(\frac{N}{2}\right)^2 \mathbb{E}\left\{ \left[h_{1,1}\eta_{1,1}^*(\hat{\mu}) + h_{1,1}^*\eta_{1,2}(\hat{\mu}) \right]^* \times \left[h_{1,1}\eta_{1,1}^*(\hat{\mu}) + h_{1,1}^*\eta_{1,2}(\hat{\mu}) \right] \right\}. \tag{17}$$

The noise term in (17) can be transformed into $\mathbb{E}\left\{\eta^*_{1,m}(\hat{\mu})\eta_{1,n}(\hat{\mu})\right\} = \frac{N\sigma^2}{2}\delta(m-n)$ due to the independence of the noise variables. CSI of the flat fading channel is considered constant within one OFDM symbol. Then $\mathbb{E}\{h_{1,1}\eta^*_{1,i}(\hat{\mu})\} = h_{1,1}\mathbb{E}\{\eta^*_{1,i}(\hat{\mu})\}$. Eq. (17) can be rewritten as

$$\begin{aligned}\mathbb{E}\{V^2\} &= \left(\frac{N}{2}\right)^2 |h_{1,1}|^2 \,\mathbb{E}\left\{|\eta_{1,1}(\hat{\mu})|^2 + |\eta_{1,2}(\hat{\mu})|^2\right\} \\ &= \left(\frac{N}{2}\right)^2 N\sigma^2 |h_{1,1}|^2 . \end{aligned} \tag{18}$$

Combining the result in (17) and the distribution of $|h_{i,k}|^2$ in (2), we obtain the closed-form expression for the correct timing probability $P(Z>1)$ as

$$P_{1\times 1}\left(|h_{1,1}|^2 > \frac{N\sigma^2}{N^2/4} = \frac{4\sigma^2}{N}\right) = e^{-\frac{4\sigma^2}{N}}. \tag{19}$$

For the normalized fading channel power and the signal power, (19) can be expressed as the function of the signal to noise ratio (SNR):

$$\begin{aligned}P_{1\times 1}\left(|h_{1,1}|^2 > \frac{4}{N}\frac{1}{\mathrm{SNR}}\right) &= e^{-\frac{4}{N}\frac{1}{\mathrm{SNR}}} \\ &\approx 1 - \frac{4}{N}\frac{1}{\mathrm{SNR}} + o\left(\frac{1}{\mathrm{SNR}}\right).\end{aligned} \tag{20}$$

where $o\left(\frac{1}{\mathrm{SNR}}\right)$ represents the higher order noise term and has the property $\lim_{x\to x_0} o(f(x))/f(x) = 0$. In (20), $\mathrm{SNR}\times\frac{N}{4}$ is the effective SNR and the gain $\frac{N}{4}$ is generated by the synchronization sequence with the length $\frac{N}{2}$. Assuming the signal power is one, $\frac{1}{\mathrm{SNR}}$ is equal to the noise power σ^2. The correct timing probability of 1×1 configuration is enhanced as the noise power decreases.

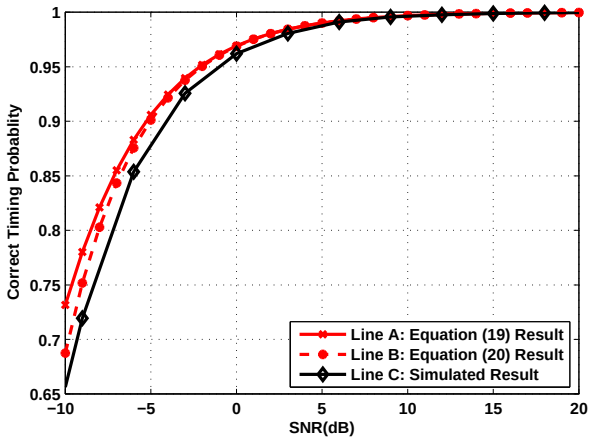

Fig. 4. CTP comparisons for 1×1 antenna configuration

Fig. 4 shows the performance of CTP with 1×1 antenna configuration in the flat fading channel. The simulation parameters are listed in Table I. 100 drops and 1000 frames in each drop are performed. Line A and Line B are the theoretical performance of CTP according to (19) and (20) respectively. Line B is the approximation of Line A. Line C is the simulation performance of CTP. Fig. 4 shows that all of the results (Line A, B and C) are very close. As SNR increases, simulation result (Line C) overlaps the theoretical results (Line A and Line B), which validates that the mathematical expression we derive for CTP can reflect its performance effectively.

B. $\forall$ N_t and $\forall$ N_r with ST/MRC

According to (10), the timing metric for each receive antenna is added in order to form MRC. Then the absolute value of the timing metric with ST/MRC is derived as

$$\begin{aligned}|M_{\mathrm{MRC}}(\mu)| = \Bigg| &\underbrace{\left(\frac{N}{2}\right)^2 \sum_{k=1}^{N_r} |h_{i_{\mathrm{ST}},k}|^2 \,\delta(\mu-\hat{\mu}) + o(\eta(\mu))}_{\text{useful signal}} \\ &+ \underbrace{\frac{N}{2}\sum_{k=1}^{N_r}\left[h_{i_{\mathrm{ST}},k}\eta^*_{k,1}(\mu) + h^*_{i_{\mathrm{ST}},k}\eta_{k,2}(\mu)\right]\delta(\mu-\hat{\mu})}_{1_{\mathrm{st}}-\text{order noise}}\Bigg|,\end{aligned} \tag{21}$$

where the second order noise $\sum_{k=1}^{N_r}\eta^*_{k,1}(\mu)\eta_{k,2}(\mu) \triangleq o(\eta(\mu))$ is omitted in the analysis, since it is a higher order complex gaussian random variable. Similar to the analysis in $N_t = N_r = 1$ case, the new random variable is defined as:

$$Z = \frac{\left(\frac{N}{2}\right)^2\left(\sum_{k=1}^{N_r}|h_{i_{\mathrm{ST}},k}|^2\right)^2}{\left|\sum_{k=1}^{N_r}\left[h_{i_{\mathrm{ST}},k}\eta^*_{k,1}(\hat{\mu}) + h^*_{i_{\mathrm{ST}},k}\eta_{k,2}(\hat{\mu})\right]\right|^2}. \tag{22}$$

We adopt the same definition of CTP as $P(Z>1)$, which means the useful signal at the correct timing shift $\hat{\mu}$ in (21) is higher than the noise. Similar to the mathematical analysis in case A, we utilize the statistic value of the denominator $V^2 = \left|\sum_{k=1}^{N_r}\left[h_{i_{\mathrm{ST}},k}\eta^*_{k,1}(\hat{\mu}) + h^*_{i_{\mathrm{ST}},k}\eta_{k,2}(\hat{\mu})\right]\right|^2$ to make the calculation of the distribution Z tractable, which is presented as

$$\begin{aligned}\mathbb{E}\{V^2\} = \mathbb{E}\Bigg\{&\left[\sum_{k=1}^{N_r}\left[h_{i_{\mathrm{ST}},k}\eta^*_{k,1}(\hat{\mu}) + h^*_{i_{\mathrm{ST}},k}\eta_{k,2}(\hat{\mu})\right]\right]^* \\ &\times\left[\sum_{k=1}^{N_r}\left[h_{i_{\mathrm{ST}},k}\eta^*_{k,1}(\hat{\mu}) + h^*_{i_{\mathrm{ST}},k}\eta_{k,2}(\hat{\mu})\right]\right]\Bigg\}.\end{aligned} \tag{23}$$

Due to the independent noise variables, $\mathbb{E}\left\{\eta^*_{k,m}(\hat{\mu})\eta^*_{l,n}(\hat{\mu})\right\} = \frac{N\sigma^2}{2}\delta(k-l)\delta(m-n)$. The flat fading channel indicates that $\mathbb{E}\left\{h_{i_{\mathrm{ST},k}}\eta^*_{k,m}(\hat{\mu})\right\} = h_{i_{\mathrm{ST},k}}\mathbb{E}\left\{\eta^*_{k,m}(\hat{\mu})\right\}$. $\eta_{k,m}(\hat{\mu})$ is the i.i.d. Gaussian noise with zero mean and variance $\frac{N}{2}\sigma^2$. $|\eta_{k,1}(\hat{\mu})|^2$ obeys exponential distribution with the mean $\frac{N}{2}\sigma^2$. Then (23) can be simplified

as

$$\mathbb{E}\{V^2\} = \sum_{k=1}^{N_r} |h_{i_{\mathrm{ST}},k}|^2 \, \mathbb{E}\left\{ |\eta_{k,1}(\hat{\mu})|^2 + |\eta_{k,2}(\hat{\mu})|^2 \right\} = N\sigma^2 \sum_{k=1}^{N_r} |h_{i_{\mathrm{ST}},k}|^2 . \quad (24)$$

After substituting CTP expression $P(Z>1)$ with (24), we have

$$P(Z>1) = P\left(\sum_{k=1}^{N_r} |h_{i_{\mathrm{ST}},k}|^2 > \frac{4}{N}\frac{1}{\mathrm{SNR}} \right) = 1 - \left(1 - e^{-\frac{4}{N}\frac{1}{\mathrm{SNR}}} \sum_{m=0}^{N_r-1} \frac{\left(\frac{4}{N}\frac{1}{\mathrm{SNR}}\right)^m}{\Gamma(m+1)} \right)^{N_t} \approx 1 - \frac{\left(\frac{4}{N}\frac{1}{\mathrm{SNR}}\right)^{N_r N_t}}{\left(\Gamma(N_r+1)\right)^{N_t}}. \quad (25)$$

The detailed derivation of (25) is shown in Appendix A. From (25), it can be found that CTP of $N_t \times N_r$ is proportional to the product of the number of transmit and receive antennas, which means that the full diversity gain is achieved by the proposed ST/MRC scheme.

C. $\forall\ N_t$ and $N_r = 1$ with ST only

In order to know the performance gain of ST scheme, CTP expression in (25) for $N_t \times 1$ antenna configuration can be written as

$$P(Z>1) = 1-(1-e^{-\frac{4}{N}\frac{1}{\mathrm{SNR}}})^{N_t} \approx 1-\left(\frac{4}{N}\frac{1}{\mathrm{SNR}}\right)^{N_t}. \quad (26)$$

It can be found that the CTP in (26) is proportional to the number of transmit antennas, which means that the transmitter diversity gain is achieved by ST scheme. Clearly, (26) is equal to (20) when $N_t = 1$.

D. $\forall\ N_t$ and $N_r = 1$ with maximum ratio transmitting (MRT)

In this part we compare the ST/MRC scheme with MRT for one receive antenna. In this case, after passing through the channel the two identical halves at the received antenna is represented as

$$y_1(\mu) = \frac{1}{\sqrt{N_t}} \sum_{i=1}^{N_t} h_{i,1} c_i(\mu - \hat{\mu}) + w_1(\mu), \quad (27)$$

where the factor $\frac{1}{\sqrt{N_t}}$ is used to normalize the transmit power in order to compare ST/MRC scheme and non-ST scheme fairly. $c_i(\mu-\hat{\mu})$ is the received synchronization sequence from the i-th transmit antenna. Using (27) for CTP analysis of MRT scheme, $P(Z>1)$ for $N_t \times 1$ antenna is derived as

$$P(Z>1) = P\left(\sum_{i=1}^{N_t} |h_{i,1}|^2 > \frac{4}{N}\frac{N_t}{\mathrm{SNR}} \right), \quad (28)$$

where the CTP performance of MRT scheme is proportional to $\sum_{i=1}^{N_t} |h_{i,1}|^2$, the sum of the fading channel power between the i-th transmit antenna and the receive antenna. The reason is that our proposed timing metric in (7) is directly related to the channel power. Considering the p.d.f. of $\sum_{i=1}^{N_t} |h_{i,1}|^2$ given by Eq. (7.18) in [28], CTP function of MRT scheme is derived as

$$P(Z>1) = \int_{\frac{4}{N}\frac{N_t}{\mathrm{SNR}}}^{\infty} \frac{1}{\Gamma(N_t)} x^{N_t-1} e^{-x} dx = e^{-\frac{4}{N}\frac{N_t}{\mathrm{SNR}}} \sum_{m=0}^{N_t-1} \frac{\frac{4}{N}\frac{N_t}{\mathrm{SNR}}^m}{\Gamma(m+1)} \approx 1 - \frac{{N_t}^{N_t}}{\Gamma(N_t+1)} \left(\frac{4}{N}\frac{N_t}{\mathrm{SNR}}\right)^{N_t}. \quad (29)$$

It can be shown that MRT scheme is degraded by a factor of $\frac{{N_t}^{N_t}}{\Gamma(N_t+1)} \geq 1$ compared with ST scheme in (26). Thus ST at the transmitter has the better timing performance than MRT. Meanwhile, MRT has the stringent requirement for the orthognality among synchronization sequences to achieve the performance gain. Since the timing detection range of Frank-Zadoff-Chu code with the ideal cross-correlation function is limited to $0, \ldots, N/(2N_t) - 1$, it is observed that the timing detection range decreases as the number of transmit antenna increases. Thus ST scheme is superior to MRT scheme in terms of both performance and feasibility.

E. $N_t = 1$ and $\forall\ N_r$ with MRC

In this case, we demonstrate the closed-form expression for CTP with MRC scheme at the receiver. When $N_t = 1$, (25) is the CTP performance of MRC, i.e.,

$$P(Z>1) = e^{-\frac{4}{N}\frac{1}{\mathrm{SNR}}} \sum_{m=0}^{N_r-1} \frac{\frac{4}{N}\frac{1}{\mathrm{SNR}}^m}{\Gamma(m+1)} \approx 1 - \frac{1}{\Gamma(N_r+1)} \left(\frac{4}{N}\frac{1}{\mathrm{SNR}}\right)^{N_r}. \quad (30)$$

Comparing (29) with (30), it is clear that MRC at the receiver can improve CTP performance more significantly than MRT due to the additional term $N_t^{N_t}$ in (29). This term is caused by the transmit power normalization.

F. Error Timing Probability

The performance gain of CTP with ST/MRC scheme at high SNR regimes can be quantified by the error timing probability (ETP), which is defined as

$$ETP = 1 - P(Z>1). \quad (31)$$

Then according to (26), (29) and (30), ETP for $N_t \times 1$ with ST scheme, $N_t \times 1$ with MRT scheme and $1 \times N_r$ with MRC scheme can be respectively derived as:

$$ETP_{N_t\times 1}^{\mathrm{ST}} \approx \left(\frac{4}{N}\frac{1}{\mathrm{SNR}}\right)^{N_t}, \quad (32)$$

$$ETP_{N_t\times 1}^{\mathrm{MRT}} \approx \frac{{N_t}^{N_t}}{\Gamma(N_t+1)} \left(\frac{4}{N}\frac{N_t}{\mathrm{SNR}}\right)^{N_t}, \quad (33)$$

$$ETP_{1\times N_r}^{\mathrm{MRC}} \approx \frac{1}{\Gamma(N_r+1)} \left(\frac{4}{N}\frac{1}{\mathrm{SNR}}\right)^{N_r}. \quad (34)$$

Comparing (32), (33) and (34), ETP for $1 \times N_r$ antenna configuration with MRC has the lowest error probability. It is advantageous over ST scheme when $N_r = N_t$ due to the factor $\frac{1}{\Gamma(N_r+1)}$. However, ETP for $N_t \times 1$ with ST performs better than MRT because of the factor $\frac{{N_t}^{N_t}}{\Gamma(N_t+1)}$.

IV. ST/MRC Scheme for Timing Synchronization in the Multipath Fading Channel

Section II and III have investigated the proposed ST/MRC scheme for timing synchronization in MIMO-OFDM systems under the flat fading channel. Both the theoretical and numerical analysis show that the proposed scheme is superior in this scenario. In this section, we investigate the application of the ST/MRC scheme for the timing synchronization in MIMO-OFDM systems under the multipath fading channel.

First, we formulate the multipath fading channel model. The CSI from the i-th transmit antenna to the k-th receive antenna is represented as $h_{i,k}(\tau) = \sum_{l=0}^{L-1} h_{i,k,l}\delta(\tau - \tau_l)$, where τ_l is the discrete delay of path l and L is the total path number. The ST principle under the multipath fading channel is the same as that in the flat fading channel. That implies only one out of N_t transmit antennas with the maximum total multipath channel power at the receiver is selected. In the multipath fading channel, (3) is modified as:

$$i_{\mathrm{ST}} = \arg\max_{1 \le i \le N_t} \left(T_i = \sum_{k=1}^{N_r} \sum_{l=0}^{L-1} |h_{i,k,l}|^2 \right). \tag{35}$$

The synchronization training sequence defined in (1) is transmitted over antenna i_{ST}. At the receiver, the two identical halves of the synchronization sequence for antenna k can be generalized as

$$y_k(\mu) = \sum_{l=0}^{L-1} h_{i_{\mathrm{ST}},k,l} c(\mu - \hat{\mu} - \tau_l) + w_k(\mu). \tag{36}$$

The definition of the timing metric in the multipath fading channel is identical with that in the flat fading channel referring to (7). Substituting (7) with (36), we obtain the timing metric for antenna k in the multipath fading channel as

$$\begin{aligned} \bar{M}_k(\mu) = & \underbrace{\left(\frac{N}{2}\right)^2 \sum_{l=0}^{L-1} |h_{i_{\mathrm{ST}},k,l}|^2 \delta(\mu - \hat{\mu} - \tau_l)}_{\text{useful signal}} + \underbrace{\eta^*_{k,1}(\mu)\eta_{k,2}(\mu)}_{2_{\mathrm{nd}}-\text{order noise}} \\ & + \underbrace{\frac{N}{2} \sum_{l=0}^{L-1} \left[h_{i_{\mathrm{ST}},k,l}\eta^*_{k,1}(\mu) + h^*_{i_{\mathrm{ST}},k,l}\eta_{k,2}(\mu) \right] \delta(\mu - \hat{\mu} - \tau_l)}_{1_{\mathrm{st}}-\text{order noise}} \end{aligned} \tag{37}$$

It is observed that the timing metric expression under the multipath fading channel is different from that under the flat fading channel. There are more than one peak, which locates at each delay tap. Fig. 5 presents one example of the timing metric of 1×1 antenna configuration with SNR equal to 0 dB in the multipath fading channel. The statistic parameters of the multipath channel are based on pedestrian channel B in [32] as listed in Table II. It is noted that different from Fig. 3, there are three peaks in the multipath fading channel. One of them locates at the correct timing index $\hat{\mu} = 10$ with the smaller value than the strongest path. The peaks at $\mu = 11$ and $\mu = 12$ are generated by the second to the fourth paths with the sampling delay $\tau = 1$ and $\tau = 2$. According to (37), one peak should appear at $\mu = 14$. But it attenuates below the noise level due to the deep fading. The other small peaks are not the useful signal but noise. Fig. 5 reveals that the timing estimation in the multipath fading channel has significant differences from that in the flat fading channel.

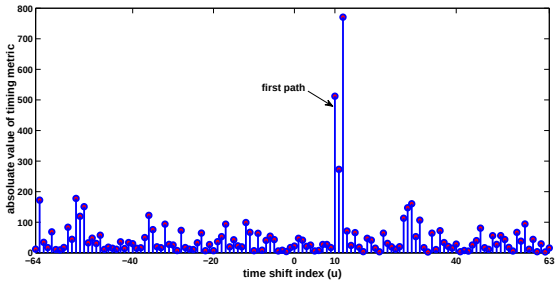

Fig. 5. One example of the absolute values of timing metric over 1×1 multipath fading channel

More importantly, Fig. 5 illustrates that each peak has the coefficient $\left(\frac{N}{2}\right)^2 |h_{i_{\mathrm{ST}},k,l}|^2$, which is proportional to the channel power of path l between the i_{ST} transmit antenna and the k-th receive antenna. Then according to the MRC scheme, the timing metric for each receive antenna is added coherently at the receiver, which is presented as:

$$\bar{M}_{\mathrm{MRC}}(\mu) = \sum_{k=1}^{N_r} \bar{M}_k(\mu). \tag{38}$$

In our simulation, the third peak corresponds to the strongest path, however we need to find the first path of the multipath fading channel. Thus the next step is to search for the timing metric peak of the first path from several peaks and to estimate the correct timing index, which is mathematically represented as:

$$\tilde{\mu} = F\left(\bar{M}_{\mathrm{MRC}}(\mu)\right) \tag{39}$$

where $F(\cdot)$ represents the method to detect the timing metric peak of the first path from several peaks in the multipath fading channel. The schemes are usually composed of the multipath delay estimation and the first path delay searching with the thresholds [30], [33], [34]. They involve setting the empirical values of the threshold. Thus it is difficult to find the closed-form expression for ETP or CTP with ST/MRC scheme under the multipath fading channel. Therefore, different from the analysis in the flat fading channel, the timing performance of the ST/MRC scheme in the multipath fading channel is validated by simulations. However, because the proposed ST/MRC scheme coherently enhances the power at the multipath delays in the timing metric (38), the SNR level is increased. Thus we could expect the ST/MRC scheme will improve the timing performance no matter what kind of detection scheme is used in (39).

V. Simulation Results and Analysis

This section investigates the performance of different antenna diversity schemes by Monte-Carlo simulations. The simulation parameters are listed in Table I.

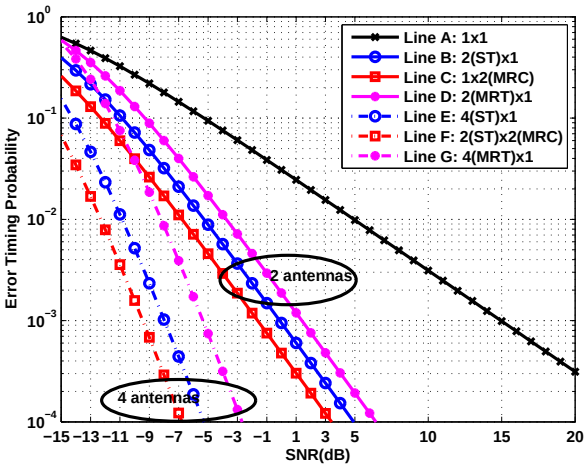

Fig. 6. Theoretical ETP comparisons for different antenna configurations

Fig. 6 demonstrates the theoretical error timing probability comparisons for different antenna configurations in the flat fading channel. It is noted that the 1×1 antenna configuration (Line A) has the highest ETP, i.e., the worst timing performance. As the number of antennas increases, ETP becomes smaller dramatically. Thus increasing the number of antennas is an effective way to enhance the timing synchronization performance in the MIMO-OFDM systems. By comparing Line B (2ST$\times$1, Eq. (32)), Line C (1$\times$2MRC, Eq. (34)) and Line D (2MRT$\times$1, Eq. (33)), we see that MRC scheme has the lowest error probability. Clearly, the number of antennas at the receiver affect the performance more significantly. It is also observed that for a given number of antennas, ST/MRC scheme (Line F) always has the best timing synchronization performance and achieves the full diversity order as shown in Eq. (25), which proves the superiority of our proposed scheme theoretically. The timing synchronization performance of ST scheme (Line B and Line E) is worse than that of ST/MRC scheme. The MRT scheme (Line D and Line G) has the worst timing synchronization performance because it requires the transmit power normalization as indicated in Eq. (29).

Fig. 7 shows the comparison between the theoretical analysis and the simulation results with different diversity schemes in the flat fading channel. Doppler filter method is utilized to produce the Channel Impulse Response (CIR) samples and the channel correlation between multiple antennas is zero [35]. 2000 drops and 1000 frames in each drop are performed. It is observed that the analytical curve and the simulation curve are closely matched for 1×1 antenna configuration (Line A and Line K), which validates our theoretical analysis. There is a gap between the analytical curves and the simulation curves for other antenna configurations. Such a gap is mainly caused by the approximation operation in order to facilitate the analysis of error or correct timing performance. That is the higher order

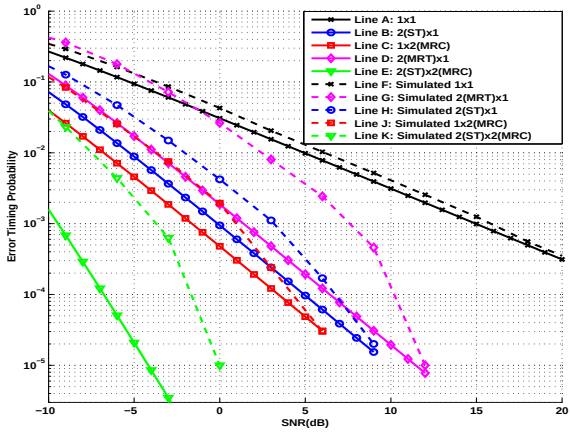

Fig. 7. Theoretical analysis and simulation ETP comparisons with different diversity schemes in the flat fading channel

noise is omitted and this operation will lead to the overestimation of the theoretical timing performance. Especially as the antenna number increases, there are more noises and such omission will introduce a slightly increased gap between the analytical and the simulation results. Moreover, it is assumed that the auto-correlation characteristic of the synchronization sequence is perfect during the analysis. But in the simulation, the large time shift of the synchronization sequence causes that only part of the synchronization training sequence is left and at the same time some of the OFDM symbols move into the correlation window. Thus the completeness of synchronization sequence is destroyed and the timing performance in the simulation becomes worse. But the analytical curves and the simulation curves are almost parallel for MRT scheme (Line B and Line G), ST scheme (Line C and Line F), MRC scheme (Line D and Line H) and ST/MRC scheme (Line E and Line J), which indicates that the analytical curves can reflect the performance of each diversity scheme in practice. Among all diversity schemes, the proposed ST/MRC scheme has the lowest ETP for both theoretical and simulation results.

Fig. 8 shows that the simulation performances of CTP with different diversity schemes in the multipath fading channel. The SCM channel model is used to produce the CIR samples. The statistic parameters of the channel are given in Table II. The power is normalized for the multiple paths. The method in [33] is utilized to detect the first path and to finish the timing estimation based on the ST/MRC scheme in (38). The empirical values of Eq. (19) in [33] are set as 20 dB and 3 dB, i.e., $\Gamma_1 = 20$ dB and $\Gamma_2 = 3$ dB. The performances of different diversity schemes in the multipath fading channel are in accordance with results in the flat fading channel. 2×1 antenna configuration with ST scheme (Line B) has better timing synchronization performance than that of 1×1 antenna configuration (Line A) because ST scheme always chooses the antenna with the highest channel power for the synchronization sequence. From the simulation, it is observed that increasing the number of the antenna is an efficient way to enhance the performance of timing synchronization especially

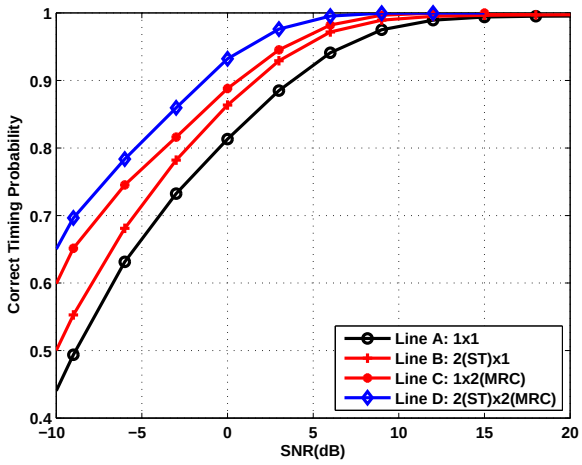

Fig. 8. Simulation CTP comparison with different diversity schemes in the multipath fading channel

increasing the number of the antenna at the receiver. Finally, we can conclude that in the multipath fading channel, the proposed ST/MRC scheme (Line D) still has the best timing synchronization performance due to the diversity gains from both the transmitter and the receiver.

VI. Conclusion

In this paper we proposed the ST/MRC scheme, which combines ST at the transmitter and MRC at the receiver to improve the timing synchronization performance of MIMO-OFDM systems in both flat fading channels and multipath fading channels. Firstly, by utilizing the statistic characteristics of the noise, we have derived the closed-form expression for correct timing probability in the flat fading channel with respect to cases: A. $N_t = 1$ and $N_r = 1$. B. $\forall\ N_t$ and $\forall\ N_r$ with ST/MRC. C. $\forall\ N_t$ and $N_r = 1$ with ST. D. $\forall\ N_t$ and $N_r = 1$ with MRT. E. $N_t = 1$ and $\forall\ N_r$ with MRC. The expression for case B reveals that CTP for ST/MRC is proportional to the product of N_t and N_r. Thus it can be concluded that our proposed ST/MRC scheme for timing synchronization can achieve the full diversity gain. The comparison between case C and case D indicates that ST scheme is advantageous over MRT because normalization of the transmit power is required for MRT. The closed-form expression for error timing probability in high SNR regimes is derived in case E. Then ST/MRC scheme is investigated in the multipath fading channel. Finally, the simulation results in both flat fading and multipath fading channels present that the theoretical analysis is in accordance with Monte-Carlo simulation results, which validates our theoretical analysis for timing synchronization with different antenna configurations and diversity schemes. The simulation results demonstrate the superiority of our proposed ST/MRC scheme over other diversity schemes because the transmitter and receiver can achieve the diversity gain simultaneously. Our proposed scheme is also attractive in practice. It can reduce the number of RF chains because only one antenna is selected at the transmitter. As a result, the system complexity is reduced.

Appendix A
Appendix derivation of (25)

Notice that CTP of ST/MRC in (25) is related to the variable $T_{i_{\mathrm{ST}},k} = \sum_{k=1}^{N_r} |h_{i_{\mathrm{ST}},k}|^2$, i.e.,

$$\begin{aligned} P(Z>1) &= P\left(\sum_{k=1}^{N_r} |h_{i_{\mathrm{ST}},k}|^2 > \frac{4}{N}\frac{1}{\mathrm{SNR}}\right) \\ &= P\left(T_{i_{\mathrm{ST}},k} > \frac{4}{N}\frac{1}{\mathrm{SNR}}\right) \\ &= \int_{\frac{4}{N}\frac{1}{\mathrm{SNR}}}^{\infty} p_{i_{\mathrm{ST}}}(x)dx, \end{aligned} \tag{40}$$

Considering the p.d.f. $p_{i_{\mathrm{ST}}}(x)$ given by (5), then we have CTP of $N_t \times N_r$ antenna configuration as

$$\begin{aligned} &P(Z>1) \\ &= \int_{\frac{4}{N}\frac{1}{\mathrm{SNR}}}^{\infty} \frac{N_t}{\Gamma(N_r)}\left(1-e^{-x}\sum_{k=0}^{N_r-1}\frac{x^k}{\Gamma(k+1)}\right)^{N_t-1} x^{N_r-1}e^{-x}dx \end{aligned} \tag{41}$$

After integration, it is further expressed as

$$\begin{aligned} P(Z>1) = &\frac{N_t}{\Gamma(N_r)}\sum_{k=0}^{N_t-1}(-1)^k\binom{N_t-1}{k}\left(\sum_{m=0}^{k(N_r-1)}\alpha_m(N_r,k)\right. \\ &\left.\times e^{-\frac{4}{N}\frac{k+1}{\mathrm{SNR}}}\sum_{j=0}^{N_r+m-1}\frac{\Gamma(j+1)\binom{N_r+m-1}{j}}{(k+1)^{j+1}}\left(\frac{4}{N}\frac{1}{\mathrm{SNR}}\right)^{N_r+m-1-j}\right). \end{aligned} \tag{42}$$

where $\binom{N_t-1}{k} = \frac{\Gamma(N_t)}{\Gamma(k+1)\Gamma(N_t-k)}$. $\alpha_m(N_r,k)$ is the coefficient of x^m after the expansion of $\left(\sum_{i=0}^{N_r-1}\frac{x^i}{\Gamma(i+1)}\right)^k$, $m \in \{0,\ldots,k(N_r-1)\}$.

Next, we give one example to show how to calculate the coefficients. By defining $f(x) = \left(\sum_{i=0}^{N_r-1}\frac{x^i}{\Gamma(i+1)}\right)^k$ and when $N_r = 3$ and $k = 2$, it is

$$f(x) = \left(\sum_{i=0}^{2}\frac{x^i}{\Gamma(i+1)}\right)^2 = \left(\frac{x^0}{\Gamma(1)}+\frac{x^1}{\Gamma(2)}+\frac{x^2}{\Gamma(3)}\right)^2. \tag{43}$$

So $\alpha_m(N_r,k)$ is the coefficient of x^m, $m \in \{0,\ldots,4\}$ as:

$$\begin{aligned} &\alpha_0(3,2) = 1,\ \alpha_1(3,2) = 2,\ \alpha_2(3,2) = 2, \\ &\alpha_3(3,2) = 1,\ \alpha_4(3,2) = 1/4. \end{aligned} \tag{44}$$

From (42), it is difficult to find the relationship between correct timing probability and the antenna number. In order to get clear understanding, we rewrite (42) as

$$\begin{aligned} P(Z>1) &= 1-\sum_{k=0}^{N_t}(-1)^k\binom{N_t}{k}e^{-\frac{4}{N}\frac{k}{\mathrm{SNR}}}\left(\sum_{m=0}^{N_r-1}\frac{\left(\frac{4}{N}\frac{1}{\mathrm{SNR}}\right)^m}{\Gamma(m+1)}\right)^k \\ &= 1-\left(1-e^{-\frac{4}{N}\frac{1}{\mathrm{SNR}}}\sum_{m=0}^{N_r-1}\frac{\left(\frac{4}{N}\frac{1}{\mathrm{SNR}}\right)^m}{\Gamma(m+1)}\right)^{N_t}. \end{aligned} \tag{45}$$

Then, the CTP has the simplified expression. We can further take advantage of $e^x = \sum_{n=0}^{\infty} \frac{x^n}{\Gamma(n+1)}$, then

$$P(Z>1) = 1 - \left\{ 1 - e^{-\frac{4}{N}\frac{1}{\mathrm{SNR}}} \left[e^{\frac{4}{N}\frac{1}{\mathrm{SNR}}} - \frac{\left(\frac{4}{N}\frac{1}{\mathrm{SNR}}\right)^{N_r}}{\Gamma(N_r+1)} + o\left(\left(\frac{1}{\mathrm{SNR}}\right)^{N_r}\right) \right] \right\}^{N_t} \approx 1 - \frac{\left(\frac{4}{N}\frac{1}{\mathrm{SNR}}\right)^{N_r N_t}}{\left(\Gamma(N_r+1)\right)^{N_t}}. \tag{46}$$

Finally, the result in (25) is derived.

REFERENCES

[1] R. D. J. V. Nee and R. Prasad, *OFDM for Wireless Multimedia Communications*. Artech House Incorporated, 2000.

[2] *IEEE Standard for Local and Metropolitan Area Networks - Part 16: Air interface for Broadband Wireless Access Systems*, IEEE Std. 802.16, 2009.

[3] *IEEE Standard for Local and Metropolitan Area Networks - Part 11: Wireless LAN Medium Access Control (MAC) and Physical Layer (PHY) Specifications*, IEEE Std. 802.11, 2007.

[4] *Radio broadcasting systems: Digital audio broadcasting (DAB) to mobile, portable and fixed receivers*, ETSI Std. ETS 300 401, 1995.

[5] *Digital video broadcasting (DVB): Frame structure, channel coding and modulation for gigital terrestrial television (DVB-T)*, ETSI Std. ETS 300 744, 1997.

[6] G. L. Stuber, J. R. Barry, S. W. McLaughlin, Y. Li, M. A. Ingram, and T. G. Pratt, "Broadband MIMO-OFDM wireless communications," *Proceedings of the IEEE*, vol. 92, no. 2, pp. 271–294, Feb. 2004.

[7] L. W. L. L. Hanzo, Y. Akhtman and M. Jiang, *MIMO-OFDM for LTE, WiFi and WiMAX: Coherent versus Noncoherent and Cooperative Turbo-Transceivers*. Wiley Press, 2010.

[8] J.-S. Baek and J.-S. Seo, "Efficient pilot patterns and channel estimations for MIMO-OFDM systems," *IEEE Transactions on Broadcasting*, vol. 58, no. 4, pp. 648–653, Dec. 2012.

[9] W. Ding, F. Yang, C. Pan, L. Dai, and J. Song, "Compressive sensing based channel estimation for OFDM systems under long delay channels," *IEEE Transactions on Broadcasting*, vol. 60, no. 2, pp. 313–321, June 2014.

[10] S. Boumard and A. Mammela, "Robust and accurate frequency and timing synchronization using chirp signals," *IEEE Transactions on Broadcasting*, vol. 55, no. 1, pp. 115–123, Mar. 2009.

[11] Y. H. You, J. Kim, and H. Song, "Pilot-assisted fine frequency synchronization for OFDM-Based DVB receivers," *IEEE Transactions on Broadcasting*, vol. 55, no. 3, pp. 674–678, Sept. 2009.

[12] M. Morelli, C. J. Kuo, and M. Pun, "Synchronization techniques for orthogonal frequency division multiple access (OFDMA): A tutorial review," *Proceedings of the IEEE*, vol. 95, no. 7, pp. 1394–1427, Jul. 2007.

[13] J. J. van de Beek, M. Sandell, and P. O. Borjesson, "ML estimation of time and frequency offset in OFDM systems," *IEEE Transactions on Signal Processing*, vol. 45, no. 7, pp. 1800–1805, Jul. 1997.

[14] T. M. Schmidl and D. C. Cox, "Robust frequency and timing synchronization for OFDM," *IEEE Transactions on Communications*, vol. 45, no. 12, pp. 1613–1621, Dec. 1997.

[15] H. A. Ziabari and M. G. Shayesteh, "Robust timing and frequency synchronization for OFDM systems," *IEEE Transactions on Vehicular Technology*, vol. 60, no. 8, pp. 3646–3656, Oct. 2011.

[16] C. Li and W. Hu, "Super-imposed training scheme for timing and frequency synchronization in OFDM systems," *IEEE Transactions on Broadcasting*, vol. 53, no. 2, pp. 574–583, Jun. 2007.

[17] P. H. Moose, "A technique for orthogonal frequency division multiplexing frequency offset correction," *IEEE Transactions on Communications*, vol. 42, no. 10, pp. 2908–2914, Oct. 1994.

[18] J. Zhang, H. Rohling, and P. Zhang, "Analysis of ICI cancellation scheme in OFDM systems with phase noise," *IEEE Transactions on Broadcasting*, vol. 50, no. 2, pp. 97–106, Jun. 2004.

[19] T. C. W. Schenk and V. van Zelst, "Frequency synchronization for MIMO OFDM wireless LAN systems," in *Proc. IEEE Vehicular Technology Conference*, Oct. 2003, pp. 781–785.

[20] A. Czylwik, "Synchronization for systems with antenna diversity," in *Proc. IEEE Vehicular Technology Conference*, Amsterdam, Sept. 1999, pp. 728–732.

[21] T. J. Liang, X. Li, R. Irmer, and G. Fettweis, "Synchronization in OFDM-based WLAN with transmit and receive diversities," in *Proc. IEEE Personal, Indoor and Mobile Radio Communications*, Berlin, Sept. 2005, pp. 740–744.

[22] M. Schellmann, V. Jungnickel, and C. V. Helmolt, "On the value of spatial diversity for the synchronisation in MIMO-OFDM systems," in *Proc. IEEE Personal, Indoor and Mobile Radio Communications*, Berlin, Sept. 2005, pp. 201–205.

[23] X. Zhou, F. Yang, and J. Song, "Novel transmit diversity scheme for TDS-OFDM system with frequency-shift m-sequence padding," *IEEE Transactions on Broadcasting*, vol. 58, no. 2, pp. 317–324, June 2012.

[24] C. Nie, Z. Tao, N. B. Mehta, A. F. Molisch, J. Zhang, T. Kuze, and S. Panwar, "Antenna selection for next generation IEEE 802.16 mobile stations," in *Proc. IEEE International Conference on Communications*, Beijing, China, May 2008, pp. 3457–3462.

[25] Z. Chen, J. Yuan, and B. Vucetic, "Analysis of transmit antenna selection/maximal-ratio combining in rayleigh fading channels," *IEEE Transactions on Vehicular Technology*, vol. 54, no. 4, pp. 1312–1321, July 2005.

[26] A. F. Molisch and M. Z. Win, "MIMO systems with antenna selection," *IEEE Microwave Magazine*, vol. 5, no. 1, pp. 46–56, Mar. 2004.

[27] S. Thoen, L. V. der Perre, B. Gyselinckx, and M. Engels, "Performance analysis of combined transmit-SC/receive-MRC," *IEEE Transactions on Communications*, vol. 49, no. 1, pp. 5–8, Jan. 2001.

[28] A. Goldsmith, *Wireless Communication*. Cambridge University Press, 2005.

[29] H. Su and J. Zhang, "Cell search algorithms for the 3G long-term evolution," *The Journal of China Universities of Posts and Telecommunications*, vol. 14, no. 2, pp. 33 – 37, June 2007.

[30] J. Bai, J. Zhang, and P. Zhang, "Timing and multipath delay estimation for a MIMO-OFDM system," *Journal of Beijing University of Posts and Telecommunications*, vol. 28, no. 5, pp. 52–54, Oct. 2005.

[31] *Spatial channel model for multiple input multiple output (MIMO) simulations*, 3GPP Std. TR 25.996 V7.0.0, 2007.

[32] *Guidelines for evaluation of radio transmission technologies for IMT-2000*, ITU-R Std. M.1225.

[33] B. Yang, K. B. Letaief, R. S. Cheng, and Z. Cao, "Timing recovery for OFDM transmission," *IEEE Journal on Selected Areas in Communications*, vol. 18, no. 11, pp. 2278–2291, Nov. 2000.

[34] E. Zhou, X. Zhang, H. Zhao, and W. Wang, "Synchronization algorithms for MIMO OFDM systems," in *Proc. IEEE Wireless Communications and Networking Conference*, Mar. 2005, pp. 18–22.

[35] *LTE Throughput Stability Dependencies on the Initial States of Different Channel Model Implementations*, 3GPP Std. R4-114 189, August 2011.

TABLE I
THE SIMULATION PARAMETERS

Terms	Values
Carrier frequency f_c	2 GHz
Bandwidth B	1.28 MHz
Subcarrier spacing Δf_c	10 kHz
Subcarrier number N	128
OFDM symbol length T_s	100 μs
Cyclic prefix length T_{CP}	3.125 μs
Length of training code	64

TABLE II
THE STATISTIC PARAMETERS OF THE MULTIPATH FADING CHANNEL

Terms	Values
Path number	6
Power (dB)	[0 -0.9 -4.9 -8.0 -7.8 -23.9]
Delay (ns)	[0 200 800 1200 2300 3700]
Sampled delay = floor(Delay*1.28MHz)	[0 0 1 1 2 4]